Damage Identification of Functionally Graded Beams using Modal Flexibility Sensitivity-based Damage Index

Du Dinh-Cong[1,2], Phat Nguyen-Huynh[1], Sy-Ngoc Nguyen[3], Trung Nguyen-Thoi[4,5*]

[1] Division of Construction Computation, Institute for Computational Science, Ton Duc Thang University, 19 Nguyen Huu Tho street, Tan Phong ward, Dist. 7, Ho Chi Minh City, Vietnam
[2] Faculty of Civil Engineering, Ton Duc Thang University, 19 Nguyen Huu Tho street, Tan Phong ward, Dist. 7, Ho Chi Minh City, Vietnam
[3] Department of Mathematics, University of Manchester, Oxford Road, Manchester, M13 9PL, UK
[4] Laboratory for Applied and Industrial Mathematics, Institute for Computational Science and Artificial Intelligence, Van Lang University, 69/68 Dang Thuy Tram Street, Ward 13, Binh Thanh Dist., Ho Chi Minh City, Vietnam
[5] Faculty of Mechanical – Electrical and Computer Engineering, Van Lang University, 69/68 Dang Thuy Tram Street, Ward 13, Binh Thanh District, Ho Chi Minh City, Vietnam
* Corresponding author, e-mail: trung.nguyenthoi@vlu.edu.vn

Abstract

Over the past decades, numerous damage diagnosis techniques based on modal flexibility have been studied and developed for various types of structures, but rarely for structures made of functionally graded (FG) materials. This paper aims to present the extensive applicability of a modal flexibility sensitivity-based damage index termed as MFBDI for damage identification of FG beams. The formulation of this damage index is based on the closed-form of modal flexibility sensitivity derived from the direct algebraic method. The applicability of the offered damage identification method is numerically demonstrated on a clamped-clamped FG beam and a two-span FG beam under (i) single and multiple damage cases, (ii) noise-polluted measurement data, and (iii) only the information of the first few incomplete modes. The identification results indicate that when the noise level added to the mode shape data is below 10%, the offered method can correctly localize the locations of damaged elements and approximately quantify their damage magnitudes in the FG beams. In addition, the influences of the number of used modes, damage magnitudes, and gradient index values are also investigated in the numerical simulations.

Keywords

modal flexibility, damage index, damage identification, analysis sensitivity, functionally graded beams

1 Introduction

Functionally graded (FG) materials classified as a class of advanced heterogeneous composites are usually made of ceramic and metallic components. An overview of FG materials production techniques developed in the last 30 years was recently presented by Saleh et al. [1]. Due to their special properties, FG materials have a wide variety of applications in many disciplines. FG beam-like structures are important structural components found extensively in many engineering fields such as civil, mechanical, and aeronautical engineering. Under realistic service conditions, the continuous operation of these structures without alarming the accumulation of damage is potentially dangerous. Therefore, it is necessarily undertaken to perform condition assessment of the FG beam structures and identify damages at the early stage.

Over the last three decades, a great variety of structural health monitoring (SHM) methodologies have been studied and developed for many kinds of structures. Among these, vibration-based SHM (VBSHM) approach that deals with the problem of structural damage detection and quantification has attracted significant attention in the SHM research community. Comprehensive literature reviews of this approach are given in [2–4]. Other review articles by Montalvão et al. [5] and Gomes et al. [6] discussed with a particular emphasis on applications of VBSHM approach to composite material structures. It is found that in the above literature reviews, little-to-no research work has been carried out to identify damage in structures made of FG materials. Until quite recently, a few studies have been conducted on numerical investigations on damage

identification of FG beams [7, 8]. Lu et al. [7] proposed a sensitivity-based approach based on finite element updating model for multiple-damage localization and quantification of axially FG beams. Yang et al. [8] proposed a damage detection strategy based on sensitivity analysis of element modal strain energy for locating and quantifying damage elements in FG beam-like structures.

In VBSHM approach, seeking or evolving damage-sensitive features is one of the important tasks [9–11]. Many of these damage features have been presented and summarized systematically in published review articles [2–4]. Among them, the modal flexibility constructed directly from mode shapes and natural frequencies can be served as a damage-sensitive feature. The major advantage of using the modal flexibility is that it does not require the use of complete mode shapes and is more sensitive to the first lower vibration modes [12, 13], which is highly welcomed in real measurement. It was also verified to be more sensitive to damages compared to other features (e.g., mode shape or natural frequency) [14]. Pandey and Biswas [12] first proposed the idea of using changes in modal flexibility matrix for localizing damages in a beam structure, which has drawn significant attention. Since then, worldwide researchers have devoted a lot of effort to the development and application of damage diagnosis techniques based on modal flexibility for various types of structures [15, 16, 17–24, 25–28].

Over the last years, a number of researchers have focused on calculating the sensitivity of modal flexibility related directly to structural physical parameters. For instance, Yang [29] introduced a mixed sensitivity method based on combining the sensitivities of modal flexibility and eigenvalues for damage detection in a 31-bar truss structure. Li et al. [30] proposed the concept of generalized flexibility matrix and studied its changes and sensitivity for finding the damage locations and their severities of an isotropic beam. Li et al.'s work [30] was then further improved by Liu and Li [31] who considered the boundedness of the damage severity in the solution of damage equations. It is worthy to remark that in the mentioned works, the sensitivity formulas of modal flexibility which was derived from the sensitivity of the complete flexibility (the inverse of stiffness matrix) are still relatively simple. In an effort to calculate the truncated modal flexibility sensitivity using the structural eigensolution sensitivities based on a direct algebraic method, Yan and Ren [32] introduced a closed-form sensitivity formulation of modal flexibility for localization and quantification of damage elements in isotropic beams. They demonstrated that the damage identification results from their method have less dependence on the truncated higher-order modes. Nevertheless, so far, its ability and effectiveness for structures made of composite structures have not yet been reported.

Basing on the research gaps mentioned above, the present work extends the modal flexibility sensitivity-based damage index termed as MFBDI for damage identification of FG beams, which is essentially an extension of the work by Yan and Ren [32]. When the modal flexibility sensitivity is calculated in [32], the first few complete mode shapes are needed. However, it will not be practical and impossible if measurements of all DOFs on the studied structure are required. To meet this requirement, iterated improved reduction system (IIRS) reduction technique [33] is employed here to expand the measured ones to a full set of mode shapes. Numerical examples including a clamped-clamped FG beam and a two-span FG beam are investigated to test the performance of the proposed damage index. For each FG beam, several hypothetical damage scenarios are designed in different locations and damage magnitudes. The effects of various noise levels, damage magnitudes, and gradient index values are also demonstrated to show how well this proposed index can perform in the damage predictions.

2 MFBDI formulation
This section presents the formulation of MFBDI [32], which will be extensively applied to FG beams. First, the change in modal flexibility is established. Then, the sensitivity analysis of modal flexibility is formulated.

2.1 Modal flexibility change
Assuming a structural system with N degree-of-freedoms (DOFs), the true flexibility matrix of the structure can be determined using vibration characteristics derived from the analytical stiffness matrix (K) and mass matrix (M):

$$\bar{F} = \bar{\Phi} \, \Lambda^{-1} \bar{\Phi}^T , \tag{1}$$

where $\Phi \in R^{(N \times N)}$ is the mass-normalized mode shape matrix, and Λ^{-1} is the diagonal matrix of natural frequencies squared.

In real testing, it is always impossible to measure all vibration modes of the structure. In other words, only a limited number of lower vibration modes are measurable. In such cases, we can approximately estimate the modal flexibility matrix of the structure using the truncated lower modes (mode shapes and modal frequencies).

Considering the first few *nmod*-vibration modes, the modal flexibility matrix of a healthy and damaged structure ($\boldsymbol{F}$ and $\boldsymbol{F}^d$) is expressed as

$$\boldsymbol{F} = \sum_{r=1}^{nmod} \frac{1}{\lambda_r} \underbrace{\boldsymbol{\Phi}_r \boldsymbol{\Phi}_r^T}_{F_r} = \sum_{r=1}^{nmod} \boldsymbol{F}_r, \ r = (1, 2, \dots, nmod), \quad (2)$$

$$\boldsymbol{F}^d = \sum_{r=1}^{nmod} \frac{1}{\left(\lambda_r^d\right)} \underbrace{\boldsymbol{\Phi}_r^d \left(\boldsymbol{\Phi}_r^d\right)^{\mathrm{T}}}_{F_r^d} = \sum_{r=1}^{nmod} \boldsymbol{F}_r^d, \quad (3)$$

where λ_r and $\boldsymbol{\Phi}_r$ are, respectively, the *r*th eigenvalue and eigenvector. One should mention herein that the eigenvector from a dynamic test is usually available and measurable with incomplete or missing components due to economic limitations and/or limited measurement points. To remedy this drawback, it is possible to employ well-established model-order reduction methods like iterated improved reduced system (IIRS) [33] to relate the master (measured) part to a full set of eigenvector through a coordinate transformation:

$$\boldsymbol{\Phi}_r^d = \left\{ \begin{array}{c} \boldsymbol{\Phi}_{r,m}^d \\ \boldsymbol{\Phi}_{r,s}^d \end{array} \right\} = \boldsymbol{T}_{IIRS} \boldsymbol{\Phi}_{r,m}^d, \quad (4)$$

where $\boldsymbol{T}_{IIRS}$ is the coordinate transformation from the master part to the full set of the eigenvector, and its detailed formulas were presented in [24, 33]; the subscripts *s* and *m* are the slave and master DOFs respectively.

From Eqs. (2) and (3), a modal flexibility change ($\Delta \boldsymbol{F}$) formulated in terms of comparing the flexibility matrix components before and after damage is defined as follows

$$\Delta \boldsymbol{F}_r = \sum_{r=1}^{nmod} \left(\boldsymbol{F}_r^d - \boldsymbol{F}_r \right). \quad (5)$$

2.2 MFBDI sensitivity
As well known, any changes in structural physical properties due to damage will influence on dynamic characteristics, thereby resulting in modal flexibility. When a small perturbation appears in structural physical parameter *p*, the modal flexibility changes can be calculated by considering the first-order derivative of Eq. (2).

$$\frac{\partial \boldsymbol{F}}{\partial p} = \sum_{r=1}^{nmod} \frac{\partial \boldsymbol{F}_r}{\partial p} = \sum_{r=1}^{nmod} \frac{\partial}{\partial p} \left(\frac{1}{\lambda_r} \boldsymbol{\Phi}_r \boldsymbol{\Phi}_r^T \right) \quad (6)$$

The sensitivity formulation of modal flexibility for the *r*th mode with respect to *p* can be represented as

$$\frac{\partial \boldsymbol{F}_r}{\partial p} = \frac{\partial}{\partial p} \left(\frac{1}{\lambda_r} \boldsymbol{\Phi}_r \boldsymbol{\Phi}_r^T \right)$$
$$= \left[-\frac{1}{\lambda_r^2} \frac{\partial \lambda_r}{\partial p} \boldsymbol{\Phi}_r \boldsymbol{\Phi}_r^T + \frac{1}{\lambda_r} \frac{\partial \boldsymbol{\Phi}_r}{\partial p} \boldsymbol{\Phi}_r^T + \frac{1}{\lambda_r} \boldsymbol{\Phi}_r \frac{\partial \boldsymbol{\Phi}_r^T}{\partial p} \right] \quad (7)$$

After rearrangement, the modal flexibility sensitivity in Eq. (7) is split as the sum of two parts

$$\frac{\partial \boldsymbol{F}_r}{\partial p} = \left[\begin{array}{c} \frac{1}{\lambda_r} \frac{\partial \boldsymbol{\Phi}_r}{\partial p} \boldsymbol{\Phi}_r^T - \frac{1}{2\lambda_r^2} \frac{\partial \lambda_r}{\partial p} \boldsymbol{\Phi}_r \boldsymbol{\Phi}_r^T + \dots \\ \frac{1}{\lambda_r} \boldsymbol{\Phi}_r \frac{\partial \boldsymbol{\Phi}_r^T}{\partial p} - \frac{1}{2\lambda_r^2} \frac{\partial \lambda_r}{\partial p} \boldsymbol{\Phi}_r \boldsymbol{\Phi}_r^T \end{array} \right]$$

$$= \underbrace{\left[\frac{1}{\lambda_r} \frac{\partial \boldsymbol{\Phi}_r}{\partial p} \boldsymbol{\Phi}_r^T - \frac{1}{2\lambda_r^2} \frac{\partial \lambda_r}{\partial p} \boldsymbol{\Phi}_r \boldsymbol{\Phi}_r^T \right]}_{\Gamma} + \dots \quad (8)$$

$$\underbrace{\left[\frac{1}{\lambda_r} \frac{\partial \boldsymbol{\Phi}_r^T}{\partial p} \boldsymbol{\Phi}_r^T - \frac{1}{2\lambda_r^2} \frac{\partial \lambda_r}{\partial p} \boldsymbol{\Phi}_r \boldsymbol{\Phi}_r^T \right]^T}_{\Gamma^T} = \Gamma + \Gamma^T$$

The component Γ in Eq. (8) is recast into a compact form as

$$\Gamma = \left[\frac{1}{\lambda_r} \boldsymbol{I} - \frac{1}{2\lambda_r^2} \boldsymbol{\Phi}_r \left\{ \begin{array}{c} \frac{\partial \boldsymbol{\Phi}_r}{\partial p} \\ \frac{\partial \lambda_r}{\partial p} \end{array} \right\} \boldsymbol{\Phi}_r^T \right]. \quad (9)$$

As can be seen in Eq. (9), the modal flexibility sensitivity requires the calculation of the first-order derivatives of eigenvector and eigenvalue. According to Lee and Jung [34, 35], the eigenvalue and eigenvector sensitivity can be determined by

$$\left\{ \begin{array}{c} \frac{\partial \boldsymbol{\Phi}_r}{\partial p} \\ \frac{\partial \lambda_r}{\partial p} \end{array} \right\} = \underbrace{\left[\begin{array}{cc} \boldsymbol{K} - \lambda_r \boldsymbol{M} & -\boldsymbol{M}\boldsymbol{\Phi}_r \\ -\left(\boldsymbol{\Phi}_r\right)^{\mathrm{T}} \boldsymbol{M} & 0 \end{array} \right]^{-1}}_{K_{U/D}} \times \dots$$

$$\underbrace{\left[\begin{array}{c} -\left(\frac{\partial \boldsymbol{K}}{\partial p} - \lambda_r \frac{\partial \boldsymbol{M}}{\partial p} \right) \\ \frac{1}{2} \left(\boldsymbol{\Phi}_r\right)^{\mathrm{T}} \frac{\partial \boldsymbol{M}}{\partial p} \end{array} \right]}_{\Theta} \boldsymbol{\Phi}_r = \boldsymbol{K}_{U/D}^{-1} \Theta \boldsymbol{\Phi}_r. \quad (10)$$

Substituting Eq. (10) into Eq. (9), one has

$$\Gamma = \left[\frac{1}{\lambda_r} \boldsymbol{I} - \frac{1}{2\lambda_r^2} \boldsymbol{\Phi}_r \right] \left[\boldsymbol{K}_{U/D} \right]^{-1} \left[\Theta \right] \boldsymbol{\Phi}_r \boldsymbol{\Phi}_r^T. \quad (11)$$

Assuming that in the degradation process, the mass distribution is almost identical. Additionally, to simplify the sensitivity analysis, each of the *e*th structural element

assigned to design parameter named p_e is supposed to be independent of each other. With these two assumptions, the component Γ in Eq. (11) becomes

$$\Gamma = \left[\frac{1}{\lambda_r} \boldsymbol{I} - \frac{1}{2\lambda_r^2} \Phi_r \right] \left[\boldsymbol{K}_{U/D} \right]^{-1} \left[\Theta_{p_e} \right] \Phi_r \Phi_r^T , \tag{12}$$

where

$$\Theta_{p_e} = \begin{bmatrix} -\left(\displaystyle\sum_e^{Ne} \frac{\partial \boldsymbol{K}}{\partial p_e} \Delta p_e \right) \\ 0 \end{bmatrix} = \begin{bmatrix} -\Delta \boldsymbol{K} \\ 0 \end{bmatrix} . \tag{13}$$

In Eq. (13), $\Delta \boldsymbol{K}$ derived from the first-order Taylor's series represents the overall perturbation of the structural stiffness. When the stiffness of the damaged structure ($\boldsymbol{K}^d$) is unknown, $\Delta \boldsymbol{K}$ can be represented by assembling the eth element stiffness ($\boldsymbol{K}_e$) that multiplies a damage ratio ($d_e \in [0,1]$) as in the following formula

$$\Delta \boldsymbol{K} = \boldsymbol{K} - \boldsymbol{K}^d = \sum_{e=1}^{Ne} d_e \boldsymbol{K}_e , \tag{14}$$

in which N_e is the total element number of the structural FE model.

By substituting Eq. (14) into Eq. (13), we obtain

$$\Theta_{p_e} = \begin{bmatrix} \displaystyle\sum_{e=1}^{Ne} d_e \boldsymbol{K}_e \\ 0 \end{bmatrix} = \sum_{e=1}^{Ne} d_e \begin{bmatrix} \boldsymbol{K}_e \\ 0 \end{bmatrix} . \tag{15}$$

Thus, combining Eq. (15) and Eq. (12), the modal flexibility sensitivity in Eq. (8) is transformed into Eq. (16) which can be used to decide the damage ratio d_e as follows:

$$\frac{\partial \boldsymbol{F}_r}{\partial p} = \sum_{e=1}^{Ne} d_e \underbrace{\left[\begin{array}{l} \left[\frac{1}{\lambda_r} \boldsymbol{I} - \frac{1}{2\lambda_r^2} \Phi_r \right] \left[\boldsymbol{K}_{U/D} \right]^{-1} \begin{bmatrix} \boldsymbol{K}_e \\ 0 \end{bmatrix} \Phi_r \Phi_r^T + \\ + \left[\left[\frac{1}{\lambda_r} \boldsymbol{I} - \frac{1}{2\lambda_r^2} \Phi_r \right] \left[\boldsymbol{K}_{U/D} \right]^{-1} \begin{bmatrix} \boldsymbol{K}_e \\ 0 \end{bmatrix} \Phi_r \Phi_r^T \right]^T \end{array} \right]}_{\Lambda_e} \tag{16}$$

$$= \sum_{e=1}^{Ne} d_e \Lambda_e .$$

Finally, let Eq. (5) be equal to Eq. (16), one can obtain a linear system of equations

$$\underbrace{\Delta \boldsymbol{F}_r}_{\{\Delta \boldsymbol{F}\}} = \sum_{e=1}^{Ne} \underbrace{d_e}_{\{d_e\}} \underbrace{\Lambda_{er}}_{[S]} . \tag{17}$$

Then Eq. (17) can be rewritten simply as

$$[\boldsymbol{S}] \{d_e\} = \{\Delta \boldsymbol{F}\} , \tag{18}$$

where $\{\Delta \boldsymbol{F}\} \in R^{n^2}$ is the residual vector, and $[\boldsymbol{S}] \in R^{n^2 \times N_e}$ is the sensitivity matrix. As can be observed in Eq. (18), the values in $\{d_e\}$ denote the damage locations and their corresponding extents that are directly obtained by solving the linear equations. When the magnitude of damage elements is imposed the non-negative constraint, non-negative least squares method [36] identified as a particularly suitable method could yield an expected result.

3 Numerical results and discussion

In this part, the damage index MFBDI presented will be applied to diagnose the damage of two FG beam structures made of a mixture of aluminum (Al) (as metal) and alumina (Al_2O_3) (as ceramic). The material properties of these structures vary continuously and smoothly through their thickness direction, which is stated in the following power-law distribution

$$E(z) = (E_c - E_m) \left(\frac{z}{h} + \frac{1}{2} \right)^k + E_m ,$$
$$\rho(z) = (\rho_c - \rho_m) \left(\frac{z}{h} + \frac{1}{2} \right)^k + \rho_m , \tag{19}$$

where the subscripts m and c denote respectively the metal and ceramic constituents of FG beam; and k is the non-negative power-law index.

The mechanical properties (i.e., Young's modulus E, and mass density ρ) of the constituent materials (Al and Al_2O_3) used in two FG beam structures are listed in Table 1, and the gradient index k is taken to be equal to 0.3. The first structure considered is a clamped-clamped FG beam [37], which is modelled by using 16 equal-length Timoshenko beam elements. The whole model contains 17 nodes and 51 DOFs. As shown in Fig. 1(a), the geometrical dimensions of the FG beam are given by the length of $L = 1.5$ m, the width of $b = 0.1$ m, and the thickness of $h = 0.05$ m. A two-span continuous FG beam is then taken as the second one which has the same geometrical dimensions and material properties. The FE model of the second beam is shown in Fig. 1(b) and it contains 33 nodes with 99 DOFs and 32 equal-length Timoshenko beam elements.

Damage in the FG beam structures is assumed as stiffness degradation, and its location is assigned to the element number. Four different damage scenarios for each beam structure are examined under single, double, triple, and multiple damage elements. For example, for the clamped-

Table 1 Material properties of the used FGM components

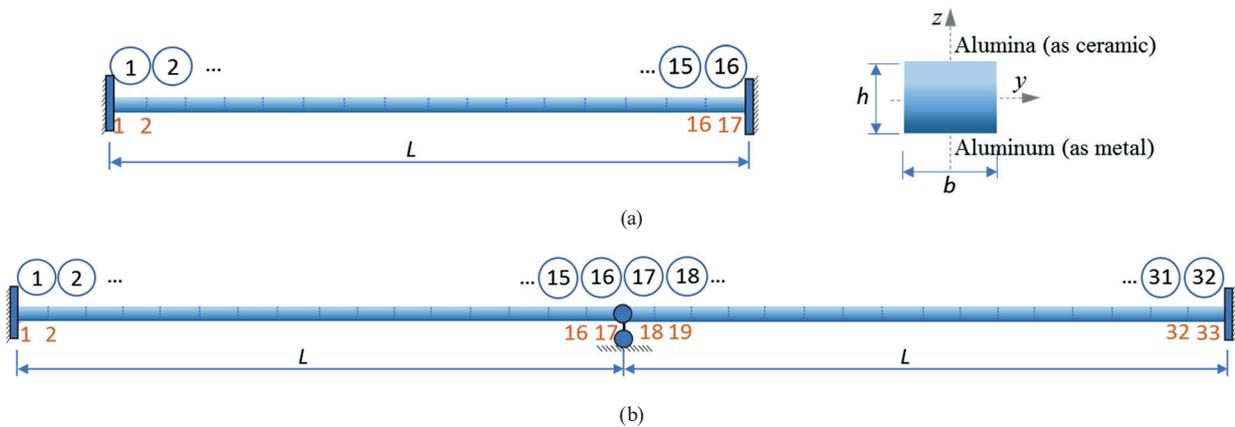| Material	Properties		
	Young's modulus (E) (MPa)	Poisson's ratio	Mass density (ρ) (kg/m³)
Aluminum (Al)	70	0.3	2700
Alumina (Al_2O_3)	380	0.3	3800

Fig. 1 Schematic of two FG beam structures; (a) Clamped-clamped FG beam, (b) Two-span continuous FG beam

clamped FG beam, scenario A represents a single damage at the clamped support that could be caused by bending moment, while scenarios B, C and D, respectively, represent double, triple and multi-damage damage scenarios that are more common with different damage locations and severities corresponding to the different maximum internal forces. The detailed information on these four scenarios is summarized in Table 2.

In this example, only the first three vibration modes are available for damage identification of two FG beam structures. Herein, due to difficulties in measuring rotational components of vibration mode shapes, it is practical to utilize only the translational DOFs for implementing the damage identification process. As such, only 30 translational DOFs of the clamped-clamped FG beam model and 60 translational DOFs of the two-span continuous FG beam model are needed. Besides, to simulate real measurement conditions, the incomplete vibration modes will be contaminated with different random noise levels. The added noise levels are imposed as follows [38, 39]

$$data^{noise} = data\left(1 + \eta(2rand - 1)\right), \qquad (20)$$

where $data$ denotes the noise-free measured eigenvalue vector or the noise-free measured eigenvector components; $data^{noise}$ denotes the measurement data polluted by an additive noise level, η. Specifically, the additive noise level of the eigenvalues is fixed at 0.5%, whereas the eigenvector components are contaminated with random noise levels ranging from 1% to 10%. Using Monte Carlo simulations, 1000 noise-polluted samples are conducted for each noise level to estimate the noise resistance capacity of the proposed damage identification method. Fig. 2 illustrates the noise distribution applied to the modal data with error levels of 3%, 5%, and 10%.

Table 2 Four different damage scenarios of the clamped-clamped FG beam

	Scenario	Damaged elements (stiffness degradation)
Clamped-clamped FG beam	A	1 (20%)
	B	5 (15%) & 16 (20%)
	C	1 (20%) & 15 (15%) & 16 (30%)
	D	1 (15%) & 2 (20%) & 5 (30%) & 6 (30%) & 14 (20%)
Two-span continuous FG beam	E	1 (20%)
	F	1 (20%) & 15 (20%)
	G	7 (20%) & 8 (15%) & 32 (20%)
	H	1 (15%) & 7 (20%) & 8 (30%) & 22 (30%) & 32 (20%)

The average damage factors calculated using the proposed index MFBDI for all damage scenarios of clamped-clamped FG beam and two-span continuous FG beam are respectively presented in Fig. 3 and Fig. 4. Here, the damage factor of each element that exceeds a preset threshold value (e.g., 0.05) is identified to be damaged. Overall, it is demonstrated that under incomplete measurement data polluted noise levels (i.e., 3%, 5%, and 10%), the proposed index MFBDI can properly identify the actual damaged location(s) in all assumed damage scenarios of both the FG beams. With regards to damage estimation, the magnitudes of the actually damaged elements obtained by the MFBDI are approximately predicted. As also shown in the figures, the trends in prediction errors increase with the increase of noise intensity from 3% to 10%. This implies that a high noise level (e.g., 10%) in the measurement data has an adverse effect on the accuracy of damage prediction results.
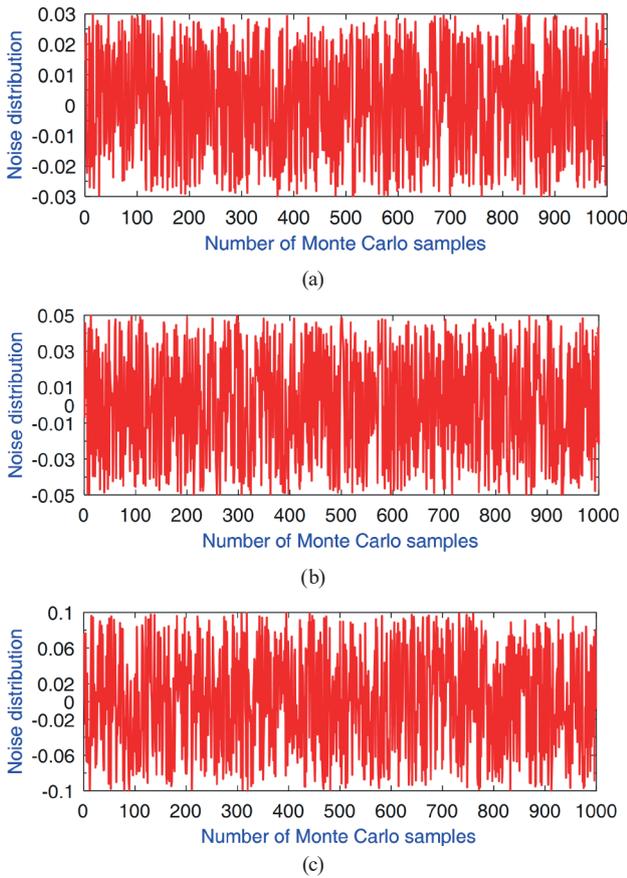
Fig. 2 Noise distribution applied to the modal data with different error levels; (a) 3% noise level, (b) 5% noise level, (c) 10% noise level

For further examination of the uncertainties in structural damage identification due to the uncertain nature of noisy measurements, the coefficient of variance (COV) is then utilized to deal with the statistical assessment of the identification results. The COV is calculated as the ratio of the standard deviation ($\bar{\sigma}_{d_e}$) to the mean ($\bar{m}_{d_e}$), which is expressed as:

$$\text{COV}(\%) = \frac{\bar{\sigma}_{d_e}}{\bar{m}_{d_e}} \times 100 \,. \tag{21}$$

The COV values for identified damage elements in each scenario of the clamped-clamped FG beam and the two-span continuous FG beam under noise levels are reported in Fig. 5 and Fig. 6, respectively. From these figures, we can observe that: (i) the values of COV increase linearly with increasing noise intensities; (ii) the element that has larger COV compared with others has more uncertainty in its damage prediction. In other words, a large COV value, e.g., element 15 in scenario C and element 7 in scenario G, are likely to give a miss-damage prediction. Therefore, when the noise level in the mode shape data is as high as 10%, the MFBDI possibly yields unreliable damage detection outcomes.
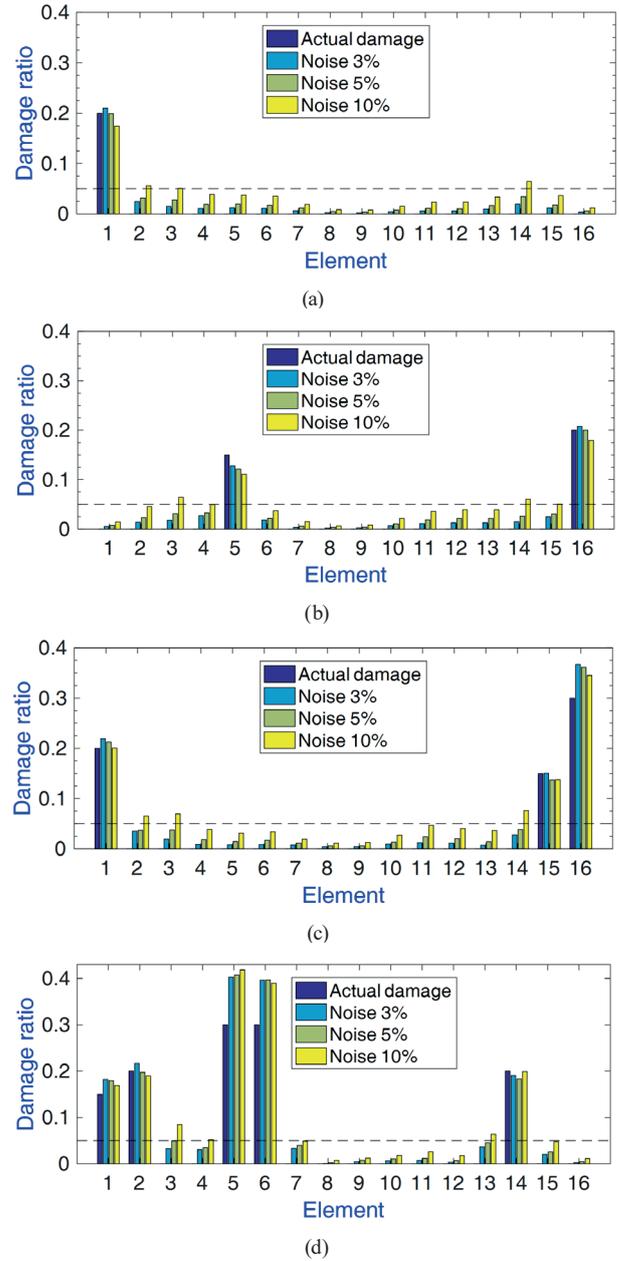
Fig. 3 Damage identification results for assumed damage cases of the clamped-clamped FG beam; (a) Scenario A, (b) Scenario B, (c) Scenario C, (d) Scenario D

Furthermore, the influences of the number of used modes, damage magnitudes, and gradient index values are successively investigated. Damage scenario A of the clamped-clamped FG beam is taken as an example for this purpose. The proposed damage index is applied to scenario A using different vibration modes (first 2, 3, and 4 modes). According to Fig. 7, although the COV values for the damaged element 1 are the same for the considered modes, it is found that better damage identification results are obtained when the minimum number of considered modes is three. Fig. 8 exhibits the COV values for
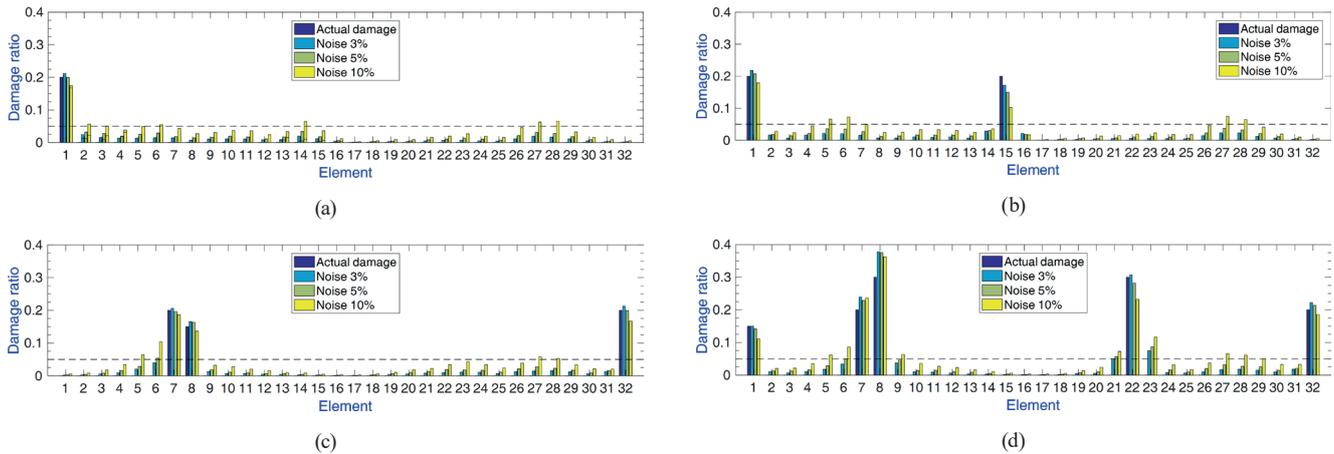
Fig. 4 Damage identification results for four assumed damage cases of the two-span continuous FG beam; (a) Scenario E, (b) Scenario F, (c) Scenario G, (d) Scenario H
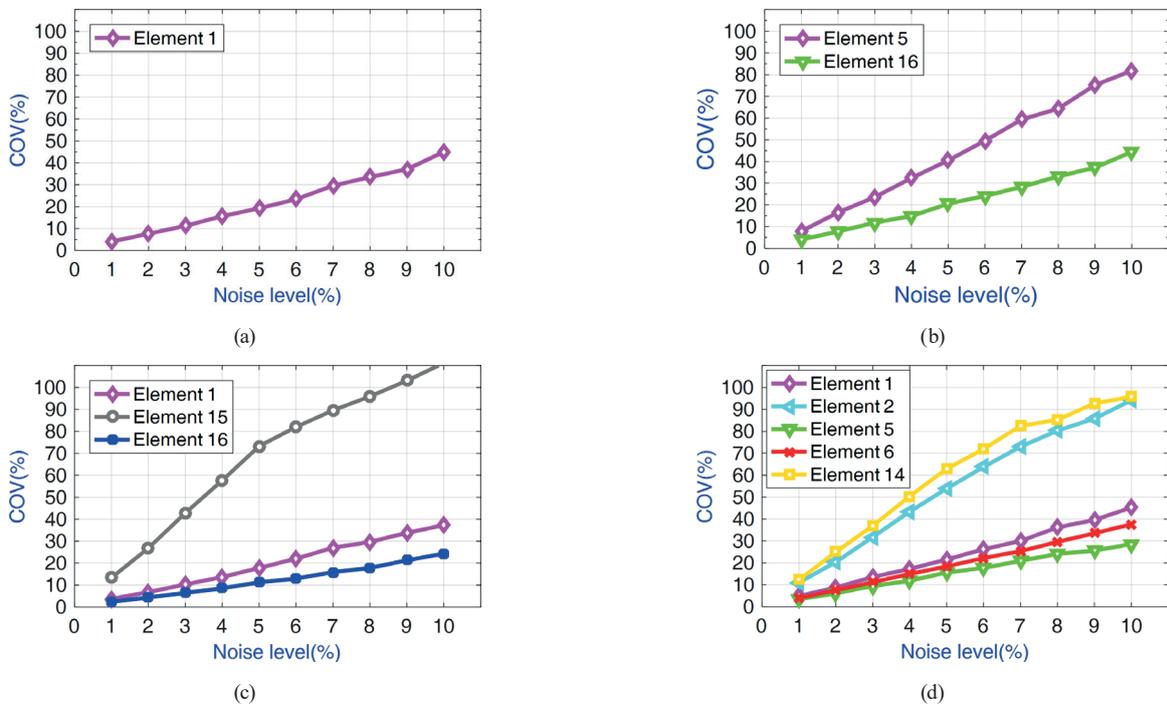

Fig. 5 COV for identified damage elements in each scenario of the clamped-clamped FG beam under noise levels; (a) Scenario A, (b) Scenario B, (c) Scenario C, (d) Scenario D

damaged element 1 when three cases of damage severities (10%, 20%, and 30%) for this element are considered. As shown in the figure, the COV decreases due to increasing the severity of damage. This means that structural element locations with a high damage level would be identified with high confidence. This can be attributed to the fact that the mode shapes change for large damage size is more significant than that for small damage size, which alleviates the adverse effects of noise.

In previous cases, the gradient index k is set to be 0.3, and now we want to investigate the influence of k on the identification results by taking different values of gradient

index, i.e., $k = 0, 1, 5,$ and 10. Fig. 9 presents damage identification results and COV values for the identified damage element of the clamped-clamped FG beam with the changed gradient index values. Both plots show the same results in term of damage localization and damage extent assessment. Thus, the gradient index k has almost no effect on the damage identification results.

4 Conclusions
This paper presents the extensive applicability of a modal flexibility sensitivity-based damage index termed as MFBDI for damage identification of FG beams. Numer-
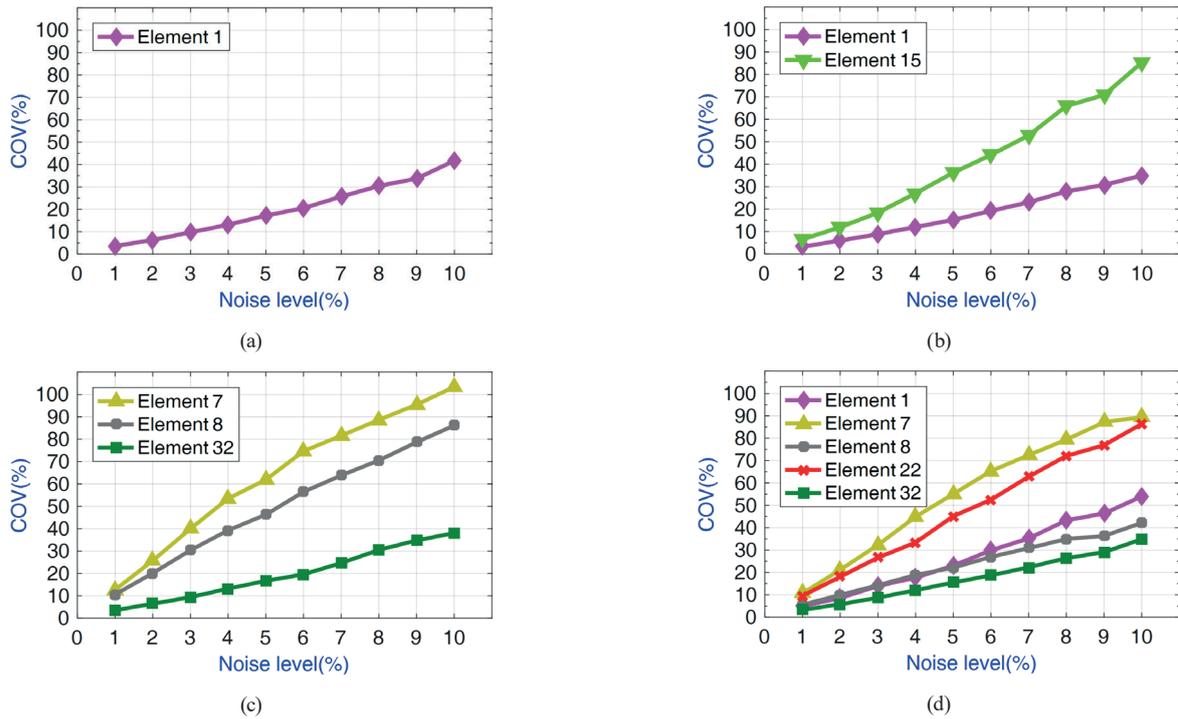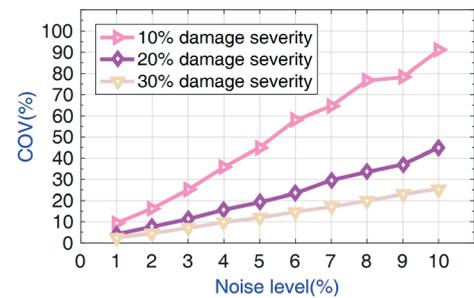
Fig. 6 COV for identified damage elements in each scenario of the two-span continuous FG beam under noise levels; (a) Scenario E, (b) Scenario F, (c) Scenario G, (d) Scenario H

(a)

(b)
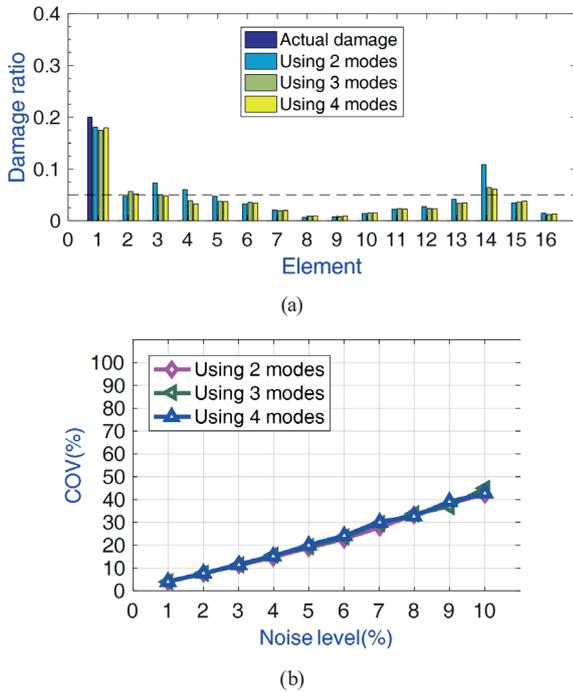
Fig. 7 (a) Damage identification results for scenario A of the clamped-clamped FG beam using different vibration modes polluted with 10% noise (first 2, 3 and 4 modes) (b) COV values for element 1

Fig. 8 COV values for element 1 with three cases of damage severities

Carlo simulations, 1000 noise-polluted samples are conducted for each noise level to discuss the noise resistance capacity of the proposed method. The damage identification results obtained in this research work reveal that when the noise level added to the mode shape data is below 10%, the MFBDI can serve as a good damage index for the FG beam structures using only the first three vibration modes. In addition to this, the statistical results indicate that the quality of the damage identification strongly depends on the number and quality of used modes as well as structural damage levels, which causes significant difficulties in its applications to real-world situations.

Acknowledgement

ical simulations of a clamped-clamped FG beam and a two-span FG beam are conducted to examine the identification capability of the proposed method. Four different damage scenarios with various noise levels in simulated incomplete modes are studied for each FG beam. Using Monte
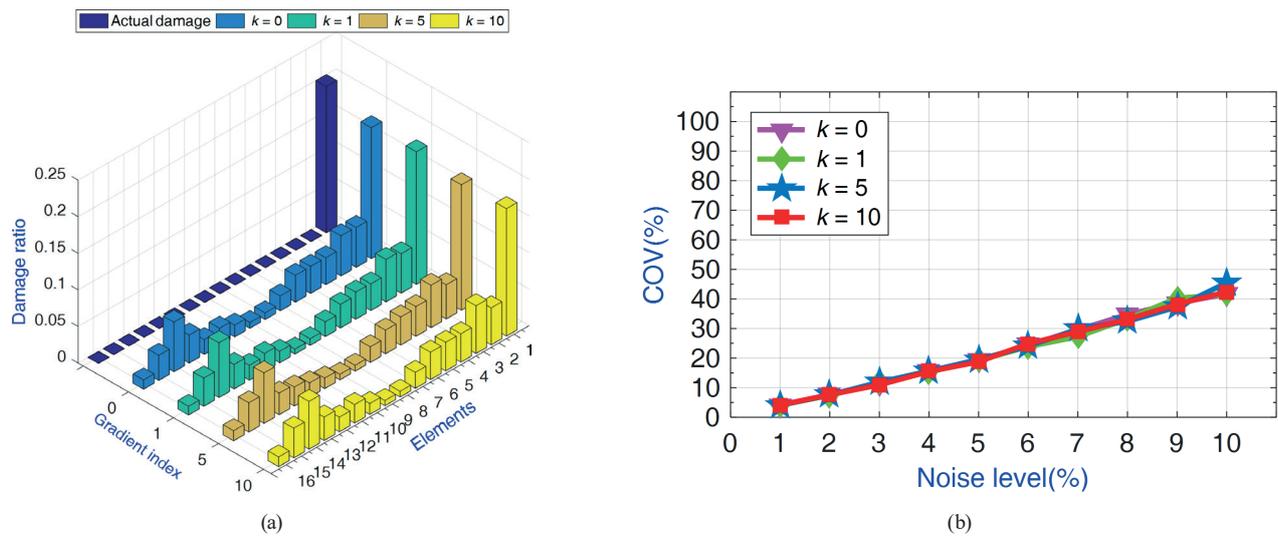
Fig. 9 (a) Damage identification results for scenario A of the clamped-clamped FG beam when gradient index $k = 0, 1, 5, 10$; (b) COV values for element 1

References

[1] Saleh, B., Jiang, J., Fathi, R., Al-hababi, T., Xu, Q., Wang, L., Song, D., Ma, A. "30 Years of Functionally Graded Materials: An Overview of Manufacturing Methods, Applications and Future Challenges", Composites Part B: Engineering, 201, 108376, 2020.
https://doi.org/10.1016/j.compositesb.2020.108376

[2] Carden, E. P., Fanning, P. "Vibration Based Condition Monitoring: A Review", Structural Health Monitoring, 3(4), pp. 355–377, 2004.
https://doi.org/10.1177/1475921704047500

[3] Fan, W., Qiao, P. "Vibration-Based Damage Identification Methods: A Review and Comparative Study", Structural Health Monitoring, 10(1), pp. 83–111, 2011.
https://doi.org/10.1177/1475921710365419

[4] Kong, X., Cai, C.-S., Hu, J. "The State-of-the-Art on Framework of Vibration-Based Structural Damage Identification for Decision Making", Applied Sciences, 7(5), 497, 2017.
https://doi.org/10.3390/app7050497

[5] Montalvão, D., Maia, N. M. M., Riberio, A. M. R. "A Review of Vibration-Based Structural Health Monitoring with Special Emphasis on Composite Materials", The Shock and Vibration Digest, 38(4), pp. 295–324, 2006.
https://doi.org/10.1177/0583102406065898

[6] Gomes, G. F., Mendéz, Y. A. D., da Silva Lopes Alexandrino, P., da Cunha Jr., S. S., Ancelotti Jr., A. C. "The Use of Intelligent Computational Tools for Damage Detection and Identification with an Emphasis on Composites – A Review", Composite Structures, 196, pp. 44–54, 2018.
https://doi.org/10.1016/j.compstruct.2018.05.002

[7] Lu, Z. R., Lin, X. X., Chen, Y. M., Huang, M. "Hybrid Sensitivity Matrix for Damage Identification in Axially Functionally Graded Beams", Applied Mathematical Modelling, 41, pp. 604–617, 2017.
https://doi.org/10.1016/j.apm.2016.09.008

[8] Yang, D., Kang, C., Hu, Z., Ye, B., Xiang, P. "On the Study of Element Modal Strain Energy Sensitivity for Damage Detection of Functionally Graded Beams", Composite Structures, 224, 110989, 2019.
https://doi.org/10.1016/j.compstruct.2019.110989

[9] Dinh-Cong, D., Nguyen-Thoi, T., Vinyas, M., Nguyen, D. T. "Two-Stage Structural Damage Assessment by Combining Modal Kinetic Energy Change with Symbiotic Organisms Search", International Journal of Structural Stability and Dynamics, 19(10), 1950120, 2019.
https://doi.org/10.1142/S0219455419501207

[10] Jahangir, H., Khatibinia, M., Masinaei, M. M. "Damage Detection in Prestressed Concrete Slabs Using Wavelet Analysis of Vibration Responses in the Time Domain", Journal of Rehabilitation in Civil Engineering, 10(3), pp. 37–63, 2022.
https://doi.org/10.22075/jrce.2021.23385.1510

[11] Daneshvar, M. H., Saffarian, M., Jahangir, H., Sarmadi, H. "Damage Identification of Structural Systems by Modal Strain Energy and an Optimization-Based Iterative Regularization Method", Engineering with Computers, 2022.
https://doi.org/10.1007/s00366-021-01567-5

[12] Pandey, A. K., Biswas, M. "Damage Detection in Structures Using Changes in Flexibility", Journal of Sound and Vibration, 169(1), pp. 3–17, 1994.
https://doi.org/10.1006/jsvi.1994.1002

[13] Pandey, A. K., Biswas, M. "Experimental Verification of Flexibility Difference Method for Locating Damage in Structures", Journal of Sound and Vibration, 184(2), pp. 311–328, 1995.
https://doi.org/10.1006/jsvi.1995.0319

[14] Zhao, J., DeWolf, J. T. "Sensitivity Study for Vibrational Parameters Used in Damage Detection", Journal of Structural Engineering, 125(4), pp. 410–416, 1999.
https://doi.org/10.1061/(ASCE)0733-9445(1999)125:4(410)

[15] Sung, S. H., Koo, K. Y., Jung, H. J. "Modal Flexibility-Based Damage Detection of Cantilever Beam-Type Structures Using Baseline Modification", Journal of Sound and Vibration, 333(18), pp. 4123–4138, 2014.
https://doi.org/10.1016/j.jsv.2014.04.056

[16] Gao, Y., Spencer Jr., B. F., Bernal, D. "Experimental Verification of the Flexibility-Based Damage Locating Vector Method", Journal of Engineering Mechanics, 133(10), pp. 1043–1049, 2007.
https://doi.org/10.1061/(ASCE)0733-9399(2007)133:10(1043)

[17] Jaishi, B., Ren, W.-X. "Damage Detection by Finite Element Model Updating Using Modal Flexibility Residual", Journal of Sound and Vibration, 290(1–2), pp. 369–387, 2006.
https://doi.org/10.1016/j.jsv.2005.04.006

[18] Yang, Q. W., Liu, J. K. "A Coupled Method for Structural Damage Identification", Journal of Sound and Vibration, 296(1–2), pp. 401–405, 2006.
https://doi.org/10.1016/j.jsv.2006.02.014

[19] Patjawit, A., Kanok-Nukulchai, W. "Health Monitoring of Highway Bridges Based on a Global Flexibility Index", Engineering Structures, 27(9), pp. 1385–1391, 2005.
https://doi.org/10.1016/j.engstruct.2005.04.003

[20] Bernal, D. "Load Vectors for Damage Localization", Journal of Engineering Mechanics, 128(1), pp. 7–14, 2002.
https://doi.org/10.1061/(ASCE)0733-9399(2002)128:1(7)

[21] Li, G.-Q., Hao, K.-C., Lu, Y., Chen, S.-W. "Flexibility Approach for Damage Identification of Cantilever-Type Structures with Bending and Shear Deformation", Computers and Structures, 73(6), pp. 565–572, 1999.
https://doi.org/10.1016/S0045-7949(98)00295-8

[22] Yang, Q. W., Liu, J. K. "Damage Identification by the Eigenparameter Decomposition of Structural Flexibility Change", International Journal for Numerical Methods in Engineering, 78(4), pp. 444–459, 2009.
https://doi.org/10.1002/nme.2494

[23] Dinh-Cong, D., Vo-Duy, T., Ho-Huu, V., Dang-Trung, H., Nguyen-Thoi, T. "An Efficient Multi-Stage Optimization Approach for Damage Detection in Plate Structures", Advances in Engineering Software, 112, pp. 76–87, 2017.
https://doi.org/10.1016/j.advengsoft.2017.06.015

[24] Dinh-Cong, D., Dang-Trung, H., Nguyen-Thoi, T. "An Efficient Approach for Optimal Sensor Placement and Damage Identification in Laminated Composite Structures", Advances in Engineering Software, 119, pp. 48–59, 2018.
https://doi.org/10.1016/j.advengsoft.2018.02.005

[25] Ahmadi-Nedushan, B., Fathnejat, H. "A Modified Teaching–Learning Optimization Algorithm for Structural Damage Detection Using a Novel Damage Index Based on Modal Flexibility and Strain Energy under Environmental Variations", Engineering with Computers, 38, pp. 847–874, 2022.
https://doi.org/10.1007/s00366-020-01197-3

[26] Hanumanthappa, S. "A New Structural Damage Detection Method for Cantilever Beam Using Generalized Flexibility Quotient Difference Method", Journal of Vibration Engineering & Technologies, 2022.
https://doi.org/10.1007/s42417-022-00655-0

[27] Das, S., Roy, K. "Structural Damage Quantification Using Flexibility Matrix-Based Approach", In: Maity, D., Patra, P. K., Afzal, M. S., Ghoshal, R., Mistry, C. S., Jana, P., Maiti, D. K. (eds.) Recent Advances in Computational and Experimental Mechanics, Vol-I, Springer, 2022, pp. 603–613. ISBN 978-981-16-6737-4
https://doi.org/10.1007/978-981-16-6738-1_49

[28] Darshan, B. U., Siddesha, H., Rajanna, T. "Structural Damage Detection for Plates Using Flexibility Based Strain Energy Method", In: Nandagiri, L., Narasimhan, M. C., Marathe, S. (eds.) Recent Advances in Civil Engineering, Springer, 2023, pp. 285-300. ISBN 978-981-19-1861-2
https://doi.org/10.1007/978-981-19-1862-9_18

[29] Yang, Q. W. "A Mixed Sensitivity Method for Structural Damage Detection", Communications in Numerical Methods in Engineering, 25(4), pp. 381–389, 2009.
https://doi.org/10.1002/cnm.1125

[30] Li, J., Wu, B., Zeng, Q. C., Lim, C. W. "A Generalized Flexibility Matrix Based Approach for Structural Damage Detection", Journal of Sound and Vibration, 329(22), pp. 4583–4587, 2010.
https://doi.org/10.1016/j.jsv.2010.05.024

[31] Liu, H., Li, Z. "An Improved Generalized Flexibility Matrix Approach for Structural Damage Detection", Inverse Problems in Science and Engineering, 28(6), pp. 877–893, 2020.
https://doi.org/10.1080/17415977.2019.1683174

[32] Yan, W.-J., Ren, W.-X. "Closed-Form Modal Flexibility Sensitivity and Its Application to Structural Damage Detection without Modal Truncation Error", Journal of Vibration and Control, 20(12), pp. 1816–1830, 2014.
https://doi.org/10.1177/1077546313476724

[33] Friswell, M. I., Garvey, S. D., Penny, J. E. T. "Model Reduction Using Dynamic and Iterated IRS Techniques", Journal of Sound and Vibration, 186(2), pp. 311–323, 1995.
https://doi.org/10.1006/jsvi.1995.0451

[34] Lee, I.-W., Jung, G.-H. "An Efficient Algebraic Method for the Computation of Natural Frequency and Mode Shape Sensitivities—Part I. Distinct Natural Frequencies", Computers & Structures, 62(3), pp. 429–435, 1997.
https://doi.org/10.1016/S0045-7949(96)00206-4

[35] Lee, I.-W., Jung, G.-H. "An Efficient Algebraic Method for the Computation of Natural Frequency and Mode Shape Sensitivities—Part II. Multiple Natural Frequencies", Computers & Structures, 62(3), pp. 437–443, 1997.
https://doi.org/10.1016/S0045-7949(96)00207-6

[36] Lawson, C. L., Hanson, R. J. "Solving Least Squares Problems", Prentice-Hall, 1974.

[37] Sina, S. A., Navazi, H. M., Haddadpour, H. "An Analytical Method for Free Vibration Analysis of Functionally Graded Beams", Materials and Design, 30(3), pp. 741–747, 2009.
https://doi.org/10.1016/j.matdes.2008.05.015

[38] Du, D.-C., Vinh, H.-H., Trung, V.-D., Hong Quyen, N.-T., Trung, N.-T. "Efficiency of Jaya Algorithm for Solving the Optimization-Based Structural Damage Identification Problem Based on a Hybrid Objective Function", Engineering Optimization, 50(8), pp. 1233–1251, 2018.
https://doi.org/10.1080/0305215X.2017.1367392

[39] Dinh-Cong, D., Pham-Toan, T., Nguyen-Thai, D., Nguyen-Thoi, T. "Structural Damage Assessment with Incomplete and Noisy Modal Data Using Model Reduction Technique and LAPO Algorithm", Structure and Infrastructure Engineering, 15(11), pp. 1436–1449, 2019.
https://doi.org/10.1080/15732479.2019.1624785